Cancer Chemother Pharmacol (2007) 59:589–601
DOI 10.1007/s00280-006-0300-z

ORIGINAL ARTICLE

In vitro anti-cancer activity and structure–activity relationships of natural products isolated from fruits of *Panax ginseng*

Wei Wang · Yuqing Zhao · Elizabeth R. Rayburn · Donald L. Hill · Hui Wang · Ruiwen Zhang

Received: 5 May 2006 / Accepted: 25 July 2006 / Published online: 22 August 2006

Abstract
Purpose *Panax ginseng* and its extracts have long been used for medical purposes; there is increasing interest in developing ginseng products as cancer preventive or therapeutic agents. The present study was designed to determine biological structure–activity relationships (SAR) for saponins present in *Panax ginseng* fruits.
Methods Eleven saponins were extracted from *P. ginseng* fruits and purified by use of D_{101} resin and ordinary and reverse-phase silica gel column chromatography. Their chemical structures were elucidated on the basis of physicochemical constants and NMR spectra. Compounds were then evaluated for SAR with their in vitro cytotoxicity against several human cancer cell lines.
Results The 11 compounds were identified as 20(*R*)-dammarane-3β,12β,20,25-tetrol (25-OH-PPD, **1)**; 20(*R*)-dammarane-3β,6α,12β,20,25-pentol (25-OH-PPT, **2**); 20(*S*)-protopanaxadiol (PPD, **3**); daucosterine **4**, 20(*S*)-ginsenoside-Rh_2 (Rh_2, **5**); 20(*S*)-ginsenoside-Rg_3 (Rg_3, **6**); 20(*S*)-ginsenoside-Rg_2 (Rg_2, **7**); 20(*S*)-ginsenoside-Rg_1 (Rg_1, **8**); 20(*S*)-ginsenoside-Rd (Rd, **9**); 20(*S*)-ginsenoside-Re (Re, **10**); and 20(*S*)-ginsenoside-Rb_1 (Rb_1, **11**). Among the eleven compounds, **1**, **3** and **5** were the most effective inhibitors of cell growth and proliferation and inducers of apoptosis and cell cycle arrest. For **1**, the IC_{50} values for most cell lines were in the range of 10–60 μM, at least twofold lower than for any of the other compounds. Compounds 1 and 3 had significant, dose-dependent effects on apoptosis, proliferation, and cell cycle progression.
Conclusions The results suggest that the type of dammarane, the number of sugar moieties, and differences in the substituent groups affect their anticancer activity. This information may be useful for evaluating the structure/function relationship of other ginsenosides and their aglycones and for development of novel anticancer agents.

Keywords *Panax ginseng* · Chemical structure · Anticancer · Structure–activity relationship

Wei Wang and Yuqing Zhao have contributed equally to this work.

W. Wang · Y. Zhao · E. R. Rayburn · D. L. Hill · H. Wang · R. Zhang (✉)
Department of Pharmacology and Toxicology,
Division of Clinical Pharmacology,
Cancer Pharmacology Laboratory,
University of Alabama at Birmingham,
Birmingham, AL 35294, USA
e-mail: ruiwen.zhang@ccc.uab.edu

D. L. Hill · H. Wang · R. Zhang
Comprehensive Cancer Center,
University of Alabama at Birmingham,
Birmingham, AL 35294, USA

Y. Zhao
Shenyang Pharmaceutical University,
Shenyang 110016, People's Republic of China

H. Wang · R. Zhang
Institute for Nutritional Sciences,
Shanghai Institutes for Biological Sciences,
Chinese Academy of Sciences,
Shanghai 200031, People's Republic of China

Introduction

For thousands of years, *Panax ginseng* (Korean ginseng) has been used in China and other Asian coun-

tries for medicinal purposes, particularly for treatment of cancer, diabetes, and heart problems [12]. There also is an increasing use of ginseng products in Western countries, with major research efforts being focused on their anti-cancer activity [10, 12]. Although numerous compounds have been isolated from the roots of the plant, the ginsenosides have shown the most activity [2, 3, 13, 18, 19, 23, 40]. Among the saponin ginsenosides are compounds with a dammarane structure, of which there are two main classes: panaxadiols (PPD) and panaxatriols (PPT) [2]. Derivatives of the primary ginsenosides are naturally generated by intestinal bacteria [1, 4, 5] and by acid hydrolysis [33].

Ginseng and compounds derived from ginseng have been reported to have a variety of anti-cancer effects. Several studies have demonstrated that ginsenosides have chemopreventive properties. Oral administration of ginseng to rats dosed with a carcinogen such as DMBA, urethane, or aflatoxin B1, reduces the incidence and size of tumors that develop [42]. Ginseng components reportedly inhibit the induction of tumors in rats dosed with MNU, ethylnitrosourea, diethylamine or DMBA [6, 39]. When applied to mouse skin, Rg_3 and protopanaxatriols inhibit the tetradecanoylphorbol acetate (TPA)-induced expression of COX-2, an effect that is attributed to inactivation of NF-κB [14]. Similarly, application of a ginseng extract with antioxidant properties reduces the number of papillomas appearing on mouse skin following tumor induction with 7,12-dimethylbenzanthracene (DMBA) and promotion with TPA [15]. In humans taking ginseng, there is a lower risk for developing cancers of the lung, oral cavity, and liver [41].

Ginseng compounds also can be used therapeutically. In mice, a glucosyl ginsenoside compound inhibited metastasis of lung carcinoma [11] and melanoma [35]. Another ginsenoside, Rb_2, inhibited angiogenesis and metastasis of melanoma cells in mice [32]. Rh_2 inhibited the growth of human ovarian cancer cells in nude mice and increased the survival of tumor-bearing mice [25]. Ginseng apparently extends postoperative survival in human patients with gastric cancer [34].

Although the mechanism(s) of action of ginsenosides are still being defined, studies of these compounds and their specific effects on tumor cells are of interest to cancer researchers. The ginsenosides Rh_1 and Rh_2, which are panaxadiols, induce differentiation of tumor cells [28]. When added to cells in culture, ginseng extracts inhibit DNA synthesis, reduce the effect of a mutagen, and diminish the effects of chemicals with transforming activity [31]. Further, several ginsenoside metabolites reduce the mutagenicity of benzo[a]pyrene [20]. Ginseng also has a radioprotective effect against radiation-induced double-strand breaks in DNA [17]. In lipopolysaccharide-stimulated macrophages, the increase in inducible nitric oxide synthase and COX-2 expression is blocked in the presence of 20(*S*)-protopanaxatriol [27]. Ginseng also has immunomodulatory activity, as evidenced by its stimulation of natural killer cells [16]. Finally, ginsenoside Rh_2 and a ginsenoside with a glucosyl moiety at the 20-position induce apoptosis in tumor cells through the activation of caspase-3 and proteolytic cleavage of poly(ADP-ribose) polymerase [21, 29]. Any or all of these mechanisms—decreased DNA synthesis, decreased susceptibility to mutation, transformation and DNA damage, decreased inflammation, increased immunosurveillance, and increased tumor apoptosis—can lead to decreased tumor growth and improved prognosis for cancer patients.

More than 60 different ginsenosides have been isolated from the leaves, stems, berries, and roots of various *Panax* species [7]. Twenty-nine of these are classified as protopanaxadiols [7]. Since different parts of ginseng plant contain different ginsenosides, administration of one part of the plant could result in pharmacological actions different from those caused by administration of another part [2]. Although several compounds present in the roots of *P. ginseng* have been identified, the fruit of this plant has not been extensively characterized.

In this report, we describe the isolation and identification of eleven ginsenoside components from *P. ginseng* fruits, seven of which had not previously been isolated from this source. We then evaluated the activities of the ginsenosides in several human cancer cell lines with diverse genetic backgrounds and elucidated the structure–activity relationships between the eleven compounds.

Materials and methods

Compound extraction and purification

The procedure for isolation and purification of the compounds is illustrated in Fig. 1. Melting points were determined on a WRS-1S digital melting point apparatus (Shanghai Precision Scientific Instrument Co. Ltd., China). ^{1}H and ^{13}C-NMR spectra were measured with an ARX 300 Spectrometer (Bruker, Germany) and chemical shifts were expressed in δ from trimethylsilane as an internal standard; mass spectra were taken on an electron-impact mass spectrometer (TSQ-7000, Finnigan); IR spectra were recorded with an IFS-55 IR spectrometer (Bruker, Germany). For

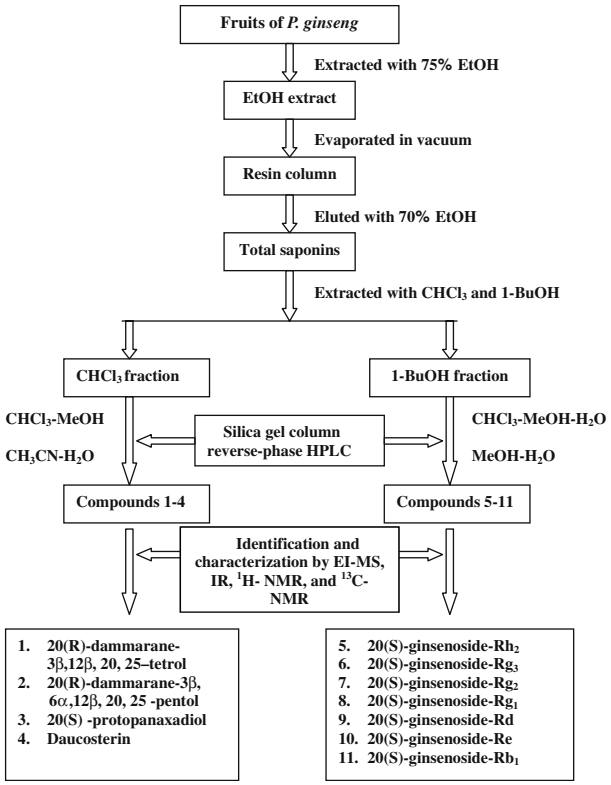

Fig. 1 Scheme for isolation and identification of compounds **1–11**

HPLC, a Shimadzu RID-6A refractive index detector was used.

For chromatography, the following were used: normal-phase silica gel column chromatography, silica gel ASTM 230–400 chromatography (Whatman Inc.); reverse-phase silica gel column chromatography, Chromatorex ODS DM1020T (Fuji Silysia Chemical, Ltd., 100–200 mesh); HPTLC-plates silica gel 60 (Merck, 0.25 mm) (normal-phase) and silica gel RP-18 F254S (Merck, 0.25 mm) (reverse-phase); reverse-phase HPTLC, pre-coated TLC plates with silica gel RP-18 WF254S (Merck, 0.25 mm). For TLC plates, detection was achieved by spraying with 10% H_2SO_4/EtOH followed by heating.

Panax ginseng fruits were obtained from Liaoning Xinbin Pharmaceutical (Fushun, China) and the identity of the fruits was confirmed by Professor Taikun Zheng (Liaoning University of Traditional Chinese Medicine). Fruits with seeds removed were extracted twice with 75% EtOH. The EtOH extract was evaporated under vacuum. Water was added to the dry material and the preparation was filtered. The solution was placed on a macro-reticular resin (D_{101}, Tianjin, China) column and eluted with 70% EtOH to yield the saponin fraction. The dried material was extracted sequentially with $CHCl_3$ and 1-BuOH. The $CHCl_3$ and 1-BuOH-soluble fractions were evaporated to dryness. The soluble materials were repeatedly subjected to column chromatography on silica gel (100 mm × 25 mm) and eluted with $CHCl_3$–1-BuOH–H_2O (10:1:1, v/v, upper layer) and $CHCl_3$–MeOH–H_2O (65:35:10, v/v, lower layer) and were further separated using semipreparative reverse-phase HPLC (250 × 10 mm, YMC-Pack ODS-A) to yield compounds **1–11**.

Identification and characterization of compounds **1–11**

The identities of each of the compounds were elucidated by comparison with known samples by their IR, ^1H and ^{13}C-NMR spectra, melting points and TLC bands on precoated silica gel 60 F_{254} (developing solvent, I, $CHCI_3$–MeOH–H_2O (65:35:10, 7:3:1, 40:10:1, v/v/v, lower phase); II, *n*-BuOH-HOAc-H_2O (4:1:2, upper phase); III, n-BuOH-HOAc-MeOH-H_2O (4:2:1: 1); spraying agent, 10% H_2SO_4 /EtOH; developed by heating at 110–120°C for 10 min).

The ginsenosides are characterized according to the number and position of sugar moieties on the dammarane-type triterpene saponin structure (Table 1). Rh_2 (Compound **5**), which has a PPD-type structure, differs from PPD (compound **3**) in that it has a glucose moiety at position C-3; Rg_3 (compound **6**) has two additional glucose moieties at the same position. Rd and Rb_1 (compounds **9** and **11**) are PPD-type saponins with three and four glucose moieties, respectively. 25-OH-PPD (compound **1**) and PPD (compound **3**) are aglycones of PPD-type ginsenosides and have the same basic structure; the difference is the variation in their side-chains (C-22-C-27). 25-OH-PPD (compound **1)** has no double bond between C-24 and C-25. Of the 20-protopanaxatriols, 25-OH-PPT (compound **2**), Rg_2 (compound **7**), Rg_1 (compound **8**) and Re (compound **10**) differ from PPD-type saponins by the presence of a hydroxyl group at C-6 (Table 1).

Biological experiments

Reagents

All chemicals and solvents were of the highest analytical grade available. Cell culture media, fetal bovine serum (FBS); phosphate-buffered saline (PBS), sodium pyruvate, non-essential amino acids, penicillin-streptomycin and other cell culture supplies were obtained from the Comprehensive Cancer Center Media Preparation Shared Facility, University of Alabama at Birmingham.

Table 1 The chemical structures of compounds **1**–**11** isolated from the fruits of *Panax ginseng*

Compound	Name	Structure	R_1	R_2
1	20(R)-dammarane-3β, 12β, 20, 25-tetrol (25-OH-PPD)	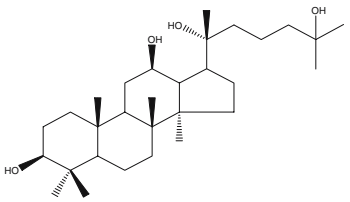		
2	20(R)-dammarane-3β, 6α, 12β, 20, 25-pentol (25-OH-PPT)	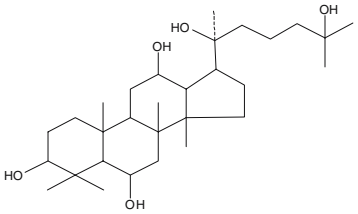		
4	β-sitosterol- 3-O-β-D-glucopyranoside (daucosterin)	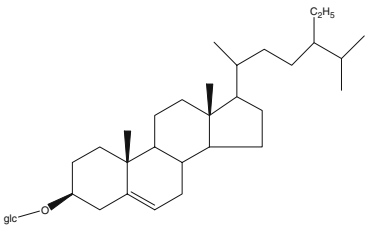		
3	20(S) -PPD	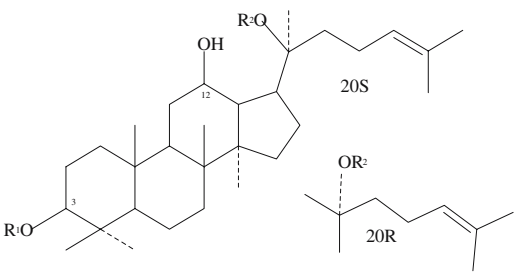 PPD-type saponin	H	H
5	20(S) -Rh_2		Glc	H
6	20(S) -Rg_3		Glc^2-Glc	H
9	20(S) –Rd		Glc^2-Glc	Glc
11	20(S) -Rb_1		Glc^2-Glc	Glc^6-Glc
7	20(S)-Rg_2	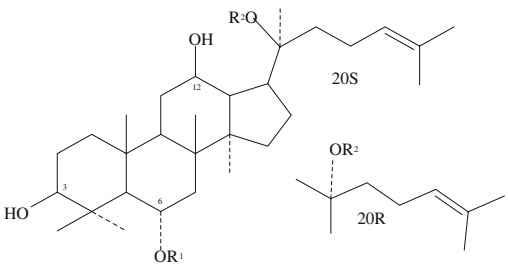 PPD-type saponin	Glc^2-Rha	H
8	20(S)-Rg_1		Glc	Glc
10	20(S)-Re		Glc^3-Rha	Glc

Cell culture

Human cancer cells were obtained from the American Type Culture Collection (Rockville, MD, USA) and cultured following their instructions. Human lung cancer cell lines used were: A549 (p53 wt), H1299 (p53 null), H838 (p53 wt) and H358 (p53 null). H838 cells were grown in RPMI 1640. H358 and H1299 cells were grown in RPMI 1640 supplemented with 1.5 g/l sodium bicarbonate, 4.5 g/l glucose, 10 mM HEPES buffer, 1 mM sodium pyruvate and 2 mM L-glutamine. A549 cells were grown in Ham's F12K medium supplemented with 2 mM L-glutamine and 1.5 g/l sodium bicarbonate. All media contained 10% FBS and 1% penicillin/streptomycin. Human prostate cancer cell lines were LNCaP (p53 wt) and PC3 (p53 null). LNCaP cells were cultured in RPMI 1640 media containing 10% FBS, 2 mM L-glutamine, 10 mM HEPES, 1 mM sodium pyruvate, glucose (4.5 mg/ml) and sodium bicarbonate (1.5 mg/ml). PC3 cells were cultured in Ham's F-12K medium containing and 2 mM L-glutamine.

Human breast cancer cell lines were MCF-7 (p53 wt) and MDA-MB-468 (p53 mt). MCF-7 cells were grown in MEM media containing 1 mM non-essential amino acids and Earle's BSS, 1 mM sodium pyruvate and 10 mg/l bovine insulin. MDA-MB-468 cells were grown in DMEM/F-12 Ham's media (DMEM/F-12 1:1 mixture). Human pancreatic cancer cell lines were HPAC (p53 wt) and PANC-1 (p53 mt). HPAC cells were grown in a 1:1 mixture of Dulbecco's modified Eagle's medium and Ham's F12 medium containing 1.2 g/l sodium bicarbonate, 2.5 mM L-glutamine, 15 mM HEPES and 0.5 mM sodium pyruvate supplemented with 2 μg/ml insulin, 5 μg/ml transferrin, 40 ng/ml hydrocortisone, 10 ng/ml epidermal growth factor and 5% fetal bovine serum. PANC-1 cells were cultured with RPMI 1640 containing 1 mM HEPES buffer, 25 μg/ml gentamicin, 1.5 g/l sodium bicarbonate, and 0.25 μg/ml amphotericin B. Human glioma cell lines were T98G (p53 mt) and A172 (p53 wt/mt). T98G cells were cultured in EMEM supplemented with 1% non-essential amino acids, and A172 cells were cultured in DMEM supplemented with 4.5 g/l of glucose. All cell culture media contained 10% FBS and 1% penicillin/streptomycin unless otherwise specified.

Cell survival assay

The effects of test compounds on human cancer cell growth, expressed as the percentage of cell survival, were determined using the MTT assay [22, 37]. The cells were grown in 96-well plates at 4–5 $\times 10^3$ cells per well and exposed to the test compounds (0, 1, 10, 25, 50, 100, 250, or 500 μM). After incubation for 72 h, 10 μL of the MTT solution (5 mg/ml; Sigma; St. Louis, MO, USA) were added into each well. The plates were incubated for 2–4 h at 37°C. The supernatant was then removed and the formazan crystals were dissolved with 100 μl of DMSO. The absorbance at 570 nm was recorded using an OPTImax microplate reader (Molecular Devices; Sunnyvale, CA, USA). The cell survival percentages were calculated by dividing the mean OD of compound-containing wells by that of DMSO-control wells. Three separate experiments were accomplished to determine the IC_{50}.

Detection of apoptosis

Following a similar protocol as above, cells in early and late stages of apoptosis were detected using an Annexin V-FITC apoptosis detection kit from BioVision (Mountain View, CA, USA), using a protocol previously reported [8, 22, 26, 36, 37, 43]. In this procedure, 2–3 $\times 10^5$ cells were exposed to the test compounds (0, 1, 5, 10, 25, or 50 μM) and incubated for 48 h prior to analysis. Cells were collected and washed with serum-free media. Cells were then re-suspended in 500 μl of Annexin V binding buffer followed by addition of 5 μl of Annexin V-FITC and 5 μl of propidium iodide (PI). The samples were incubated in the dark for 5 min at room temperature and analyzed with a Becton Dickinson FACSCalibur instrument (Ex = 488 nm; Em = 530 nm). Cells that were positive for Annexin V-FITC alone (early apoptosis) and Annexin V-FITC and PI (late apoptosis) were counted.

Cell proliferation

The effects of test compounds on cell proliferation were determined by BrdU incorporation (Oncogene, La Jolla, CA, USA), with a protocol previously reported [8, 22, 26, 36, 37]. Cells were seeded in 96-well plates (8×10^3 to 1.2×10^4 cells per well) and incubated with various concentrations of test compounds (0–50 μM) for 24 h. BrdU was added to the medium 10 h before termination of the experiment. The BrdU incorporated into cells was determined by anti-BrdU antibody, and absorbance was measured at dual wavelengths of 450/540 nm with an OPTImax microplate reader (Molecular Devices; Sunnyvale, CA, USA).

Cell cycle measurements

For determination of effects on the cell cycle, a protocol similar to that described above was used. Cells

($2–3 \times 10^5$) were exposed to the test compounds (0, 1, 5, 10, 25, or 50 μM) and incubated for 48 h prior to analysis. Cells were trypsinized, washed with PBS and fixed in 1.5 ml of 95% ethanol at 4°C overnight, followed by incubation with RNAse and staining with propidium iodide (Sigma). The DNA content was determined by flow cytometry.

Results

Extraction, isolation, and purification of ginsenosides

As illustrated in Fig. 1, compounds were extracted from fresh *P. ginseng* fruits using 75% EtOH. The extract was passed through a macro-reticular resin column and saponins were eluted with 70% EtOH. The saponins, obtained after evaporation of the EtOH, were extracted with $CHCl_3$ and 1-BuOH. These fractions were evaporated to dryness and repeatedly subjected to silica gel column and semi-preparative reverse-phase HPLC to obtain compounds **1–11** (Table 1). The compounds were identified by comparison of their physical characteristics (melting point (mp), mass spectroscopy, IR, 1H- NMR, and 13C-NMR spectra) with reported values [9, 38, 44].

Structure elucidation

Compound **1** was characterized as 20(*R*)-dammarane-3*β*,12*β*,20,25-tetrol (25-OH-PPD) based upon the following: **1** was isolated as white needle crystals, with mp 252–254°C from EtOAc. EI-MS (*m/z*): 478 for $C_{30}H_{54}O_4$,^{13}C-NMR (pyridine-d_5, 600 MHz) δ (ppm); signals of hydroxyl carbons: 79.5 (C-3), 71.9 (C-12), 74.7 (C-20), 71.5 (C-25-OH); 51.3 (C-17), 22.4 (C-21), 44.0 (C-22) (the diagnostic signals for determination of the 20R configuration). ^{13}C-NMR data for other carbons were as follows: 40.3 (C-1), 28.0 (C-2), 40.0 (C-4), 57.3 (C-5), 18.9 (C-6), 35.9 (C-7), 40.9 (C-8), 50.9 (C-9), 38.2 (C-10), 32.0 (C-11), 49.5 (C-13), 52.6 (C-14), 32.0 (C-15), 27.1(C-16), 16.3 (C-18-CH_3), 6.8 (C-19-CH_3), 19.4 (C-23), 45.4 (C-24), 29.4 (C-26-CH_3), 29.1 (C-27-CH_3), 28.6 (C-28-CH_3), 16.2 (C-29-CH_3), 17.4 (C-30-CH_3).

Compound **2** was characterized as 20(*R*)-dammarane-3*β*,6*α*,12*β*,20,25-pentol (25-OH-PPT). It was isolated from EtOAc as white needle crystals with mp 177–179°C. EI-MS (*m/z*): 494 for $C_{30}H_{54}O_5$, ^{13}C-NMR (pyridine-d_5, 600 MHz) δ (ppm): signals of hydroxyl carbons: 79.5 (C-3), 69.9 (C-6), 71.9 (C-12), 74.7 (C-20), 71.5 (C-25-OH); 50.9 (C-17), 22.4 (C-21), 44.0 (C-22) (the diagnostic signals for determination of the 20R configuration). ^{13}C-NMR data for other carbons were as follows: 40.2 (C-1), 27.8 (C-2), 40.5 (C-4), 62.1(C-5), 47.3 (C-7), 42.0 (C-8), 50.7 (C-9), 40.2 (C-10), 32.0 (C-11), 49.6 (C-13), 52.5 (C-14), 31.4 (C-15), 27.1 (C-16), 17.6 (C-18), 17.7 (C-19), 18.9 (C-23), 45.4 (C-24), 29.1 (C-26), 29.4 (C-27), 31.9 (C-28), 16.1 (C-29), 17.4 (C-30).

Compound **3** was characterized as 20(*S*)-protopanaxadiol (PPD). Compound **3** formed colorless fine crystals with mp 196–198°C from EtOAc; IR (KBr) cm^{-1}: 3,410, 1,645, 1,068 cm^{-1}; ^{1}H-NMR (pyridine-d_5, 300 MHz) δ (ppm) 0.84, 0.98, 0.98, 0.99, 1.29, 1.66, 1.63, 1.64 (3H each, all s, 3H-19, 18 , 30, 29, 28, 26, 21, 27), 5.34 (1H, m, H-24); ^{13}C-NMR (pyridine-d_5, 600 MHz) δ (ppm): signals of olefinic carbons: 126.2 (C-24), 130.5 (C-25). Signals of hydroxyl carbons: 77.8 (C-3), 70.9 (C-12), 72.9 (C-20); 54.5 (C-17), 22.8 (C-21), 35.7(C-22) (the diagnostic signals for determination of the 20S configuration). Signals of eight methyl carbons: 16.5(C-18), 16.3(C-19), 22.8 (C-21), 25.6 (C-26), 17.6 (C-27), 28.6 (C-28), 15.8 (C-29), 17.1(C-30). ^{13}C-NMR data for other carbons were as follows: 39.4 (C-1), 28.2 (C-2), 39.6 (C-4), 56.3 (C-5), 18.7 (C-6), 35.2 (C-7), 40.1 (C-8), 50.4 (C-9), 37.3 (C-10), 32.0 (C-11), 48.5 (C-13), 51.6 (C-14), 31.8 (C-15), 26.6 (C-16), 22.9 (C-23).

Compound **4** was characterized as daucosterin (*β*-sitosterol-3-*O*-*β*-D-glucopyranoside). It formed a white amorphous powder with mp 288–289°C from MeOH. IR (KBr) cm^{-1}: 3,435, 1,644, 1,078. ^{13}C-NMR (pyridine-d_5, 600 MHz) δ (ppm): signals of olefinic carbons: 41.2 (C-5), 21.7 (C-6). Signals of hydroxyl carbons: 78.2 (C-3). ^{13}C-NMR data for other carbons were as follows: 37.6 (C-1), 30.2 (C-2), 39.2 (C-4), 32.2 (C-7), 31.9 (C-8), 50.5(C-9), 36.9 (C-10), 31.3 (C-11), 8.5 (C-12), 42.7 (C-13), 56.9 (C-14), 24.5 (C-15), 40.0 (C-16), 56.4 (C-17), 12.1 (C-18), 19.3 (C-19), 36.2 (C-20), 19.1 (C-21), 34.7 (C-22), 26.8 (C-23), 46.2 (C-24), 29.6 (C-25), 19.4 (C-26), 19.8 (C-27), 28.5 (C-28), 12.0 (C-29), 102.4 (3-glc C-1′), 74.9 (C-2′), 78.4 (C-3′), 71.7(C-4′), 77.6 (C-5′), 62.9 (C-6′).

Compound **5** was characterized as 20(*S*)-dammarane-3-*O*-*β*-D-glucopyranosyl-12*β*, 20-diol (Rh_2). It formed colorless fine crystals with mp183–184°C from EtOAc. IR (KBr) cm^{-1}: 3,430, 1,644, 1,078. ^{13}C-NMR (pyridine-d_5, 600 MHz) δ (ppm): signals of olefinic carbon: 126.4 (C-24), 130.7 (C-25). Signals of hydroxyl carbons: 88.8 (C-3), 71.1 (C-12), 73.2 (C-20); 54.7 (C-17), 22.0 (C-21), 35.4 (C-22) (the diagnostic signals for determination of the 20S configuration). ^{13}C-NMR data for other carbons were as follows: 39.3 (C-1), 27.4 (C-2), 39.9 (C-4), 56.5 (C-5), 18.6 (C-6), 35.4 (C-7), 40.2 (C-8), 50.7 (C-9), 37.4 (C-10), 32.2 (C-11), 48.6 (C-13), 51.8 (C-14), 31.8 (C-15), 26.7 (C-16), 16.6 (C-18), 16.4

(C-19), 23.0 (C-23), 25.7 (C-26), 17.7 (C-27), 28.4 (C-28), 16.1 (C-29), 17.2 (C-30), 106.7 (3-glc C-1′), 75.9 (C-2′), 78.7 (C-3′), 72.2 (C-4′), 78.0 (C-5′), 63.3 (C-6′).

Compound **6** was characterized as 20(*S*)-dammarane-3-O-*β*-D-glucopyranosyl-(1 → 2)-*O*-*β*-D-glucopyranosyl-12*β*, 20-diol (Rg_3). It formed colorless fine crystals with mp 298–303°C from EtOH-1-BuOH. IR (KBr) cm^{-1}: 3,410, 1,645, 1,076. ^{1}H-NMR (pyridine-d_5, 600MHz) *δ* 0.81, 0.96, 0.96, 1.10, 1.27, 1.62, 1.62, 1.66 (3H each, all s, H3–19, 18, 30, 29, 28, 26, 21, 27), 4.89 (1H, d, *J* = 7.0 Hz, H-1′), 5.31 (1H, d-like, H-24), 5.35 (1H, d, *J* = 7.0 Hz, H-1′′). ^{13}C-NMR (pyridine-d_5, 600 MHz) *δ* (ppm): signals of olefinic carbons: 126.1 (C-24), 130.4 (C-25). Signals of hydroxyl carbons: 88.9 (C-3), 70.9 (C-12), 73.0 (C-20); 54.5 (C-17), 22.3 (C-21), 35.3 (C-22) (the diagnostic signals for determination of the 20S configuration). ^{13}C-NMR data for other carbons were as follows: 39.2 (C-1), 26.9 (C-2), 39.7 (C-4), 56.4 (C-5), 18.5 (C-6), 35.2 (C-7), 40.1 (C-8), 50.4 (C-9), 37.0 (C-10), 32.0 (C-11), 49.1 (C-13), 51.8 (C-14), 31.5 (C-15), 26.8 (C-16), 16.3 (C-18), 16.2 (C-19), 22.8 (C-23), 25.6 (C-26), 17.4 (C-27), 28.2 (C-28), 15.7 (C-29), 17.1 (C-30), 105.1 (3-glc C-1′), 83.6 (C-2′), 78.2 (C-3′), 71.7 (C-4′), 78.0 (C-5′), 62.9 (C-6′), 106.1 (C-1′′), 77.2 (C-2′′), 78.4 (C-3′′), 71.7 (C-4′′), 78.1 (C-5′′), 62.8 (C-6′′).

Compound **7** was characterized as 20(*S*)-dammarane-6-α-*O*-L-rhamnopyranosyl-(1 → 2)-*O*-*β*-D-glucopyranosyl-3*β*,12*β*,20-tetrol (Rg_2). It formed colorless fine crystals with mp 183–184°C from MeOH-EtOAc. ^{13}C-NMR (pyridine-d_5, 600 MHz) *δ* (ppm): signals of olefinic carbons: 126.4 (C-24), 130.8 (C-25). Signals of hydroxyl carbons: 78.4 (C-3), 74.4 (C-6), 70.9 (C-12), 72.7 (C-20); 54.3 (C-17), 22.6 (C-21), 35.5 (C-22) (the diagnostic signals for determination of the 20S configuration). ^{13}C-NMR data for other carbons were as follow: 39.7 (C-1), 27.8 (C-2), 40.0 (C-4), 60.9 (C-5), 46.1 (C-7), 41.2 (C-8), 49.8 (C-9), 39.4 (C-10), 31.4 (C-11), 48.9 (C-13), 51.7 (C-14), 31.3 (C-15), 26.7 (C-16), 17.2 (C-18), 17.1 (C-19), 22.8 (C-23), 25.8 (C-26), 17.9 (C-27), 28.8 (C-28), 16.6 (C-29), 17.5 (C-30), 102.0 (C-1′), 78.3 (6-glc-C-2′), 79.4 (C-3′), 73.0 (C-4′), 78.6 (C-5′), 63.2 (C-6′), 101.8 (rha C-1′′), 72.5 (C-2′′), 72.3 (C-3′′), 74.3 (C-4′′), 69.5 (C-5′′), 18.8 (C-6′′).

Compound **8** was characterized as 20(*S*)-dammarane-6-*O*-α-L-rhamnopyranosyl-20-*O*-*β*-D-glucopyranosyl-3*β*,12*β*-diol (Rg_1). It formed colorless fine crystals with mp 194–195°C from BuOH-EtOAc. ^{13}C-NMR (pyridine-d_5, 600 MHz) *δ* (ppm): signals of olefinic carbons: 126.2 (C-24), 130.6 (C-25). Signals of hydroxyl carbons: 78.4 (C-3), 77.9 (C-6), 70.8 (C-12), 83.3 (C-20); 54.6 (C-17), 22.5 (C-21), 35.9 (C-22) (the diagnostic signals for determination of the 20S configuration). ^{13}C-NMR data for other carbons were as follows: 39.5 (C-1), 27.6 (C-2), 40.1 (C-4), 61.3 (C-5), 44.9 (C-7), 41.0 (C-8), 49.9 (C-9), 39.5 (C-10), 31.8 (C-11), 48.9 (C-13), 51.6 (C-14), 31.9 (C-15), 26.9 (C-16), 17.4 (C-18), 17.2 (C-19), 23.2 (C-23), 25.7 (C-26), 17.7 (C-27), 28.5 (C-28), 16.2 (C-29), 17.0 (C-30), 106.3 (6-glc C-1′), 75.3 (C-2′), 80.0 (C-3′), 71.6 (C-4′), 79.3 (C-5′), 62.9 (C-6′), 98.1 (20-glc C-1′), 74.9 (C-2′), 78.8 (C-3′), 71.3 (C-4′), 77.8 (C-5′), 62.9 (C-6′).

Compound **9**, characterized as 20(*S*)-dammarane-3-O-*β*-D-glucopyranosyl-(1 → 2)-*O*-*β*-D-glucopyranosyl-20-*O*-*β*-D-glucopyranosyl-(1 → 6)-xylopyranosyl-12*β*-ol (Rd), formed a white amorphous powder with mp 206–209°C from EtOH-EtOAc. ^{13}C-NMR (pyridine-d_5, 600 MHz) *δ* (ppm): signals of olefinic carbons: 126.4 (C-24), 130.9 (C-25). Signals of hydroxyl carbons: 89.0 (C-3), 70.2 (C-12), 83.3 (C-20); 54.6 (C-17), 22.4 (C-21), 36.2 (C-22) (the diagnostic signals for determination of the 20S configuration). ^{13}C-NMR data for other carbons were as follows: 39.2 (C-1), 26.8 (C-2), 39.7 (C-4), 56.4 (C-5), 18.5 (C-6), 35.2 (C-7), 40.1 (C-8), 50.2 (C-9), 36.9 (C-10), 31.0 (C-11), 49.6 (C-13), 51.5 (C-14), 30.8 (C-15), 26.7 (C-16), 16.6 (C-18), 16.4 (C-19), 23.2 (C-23), 25.8 (C-26), 17.4 (C-27), 28.1 (C-28), 16.3 (C-29), 17.8 (C-30), 105.2 (3-glc C-1′), 83.6 (C-2′), 78.3 (C-3′), 71.7 (C-4′), 78.1 (C-5′), 62.9 (C-6′), 106.1 (C-1′′), 77.2 (C-2′′), 79.4 (C-3′′), 71.7 (C-4′′), 78.0 (C-5′′), 62.8 (C-6′′), 98.3 (C-1′), 75.2 (C-2′), 79.3 (20-glc1C-3′), 71.7 (C-4′), 78.1 (C-5′), 62.6 (C-6′).

Compound **10** was characterized as 20(*S*)-dammarane-6-*O*-*β*-D-rhamnopyranosyl-(1 → 2)-*O*-*β*-D-glucopyranosyl-20-*O*-*β*-D-glucopyranosyl-3*β*,12*β*-diol (Re). It formed colorless fine crystals with mp 199–201°C from MeOH-H_2O. ^{13}C-NMR (pyridine-d_5, 600 MHz) *δ* (ppm): signals of olefinic carbons: 125.8 (C-24), 130.8 (C-25). Signals of hydroxyl carbons: 78.5 (C-3), 74.0 (C-6), 70.2 (C-12), 83.3 (C-20); 54.8 (C-17), 22.3 (C-21), 36.0 (C-22) (the diagnostic signals for determination of the 20S configuration). ^{13}C-NMR data for other carbons were as follows: 39.7 (C-1), 27.5 (C-2), 39.7 (C-4), 61.0 (C-5), 45.5 (C-7), 41.2 (C-8), 49.6 (C-9), 39.7 (C-10), 30.8 (C-11), 49.1 (C-13), 51.4 (C-14), 30.8 (C-15), 26.6 (C-16), 17.3 (C-18), 17.2 (C-19), 23.1 (C-23), 25.4 (C-26), 17.6 (C-27), 29.2 (C-28), 17.0 (C-29), 17.6 (C-30), 101.3 (6-glc C-1′), 78.7 (C-2′), 77.6 (C-3′), 72.1 (C-4′), 77.6 (C-5′), 62.9 (C-6′), 101.7 (rha C-1′′), 72.1 (C-2′′), 72.2 (C-3′′), 73.9 (C-4′′), 69.3 (C-5′′), 18.3 (C-6′′), 98.0 (20-glc1 C-1′), 75.0 (C-2′), 78.7 (C-3′), 71.8 (C-4′), 78.7 (C-5′), 63.3 (C-6′).

Compound **11**, characterized as 20(*S*)-dammarane-3-*O*-*β*-D-glucopyranosyl-(1 → 2)-*O*-*β*-D-glucopyranosyl-20-O-*β*-D-glucopyranosyl-(1 → 6)-*O*-*β*-D-glucopyranosyl-12*β*-ol (Rb_1), formed a white amorphous powder with mp 198–200°C from EtOH–BuOH.

^{13}C-NMR (pyridine-d_5, 600 MHz) δ (ppm): signals of olefinic carbons: 125.8 (C-24), 130.8 (C-25). Signals of hydroxyl carbons: 89.3 (C-3), 70.3 (C-12), 83.5 (C-20); 54.7 (C-17), 22.6 (C-21), 36.1 (C-22) (the diagnostic signals for determination of the 20S configuration). ^{13}C-NMR data for other carbons were as follows: 39.3 (C-1), 26.6 (C-2), 39.6 (C-4), 56.3 (C-5), 18.5 (C-6), 35.1 (C-7), 39.9 (C-8), 50.3 (C-9), 36.8 (C-10), 30.7 (C-11), 49.3 (C-13), 51.3 (C-14), 30.8 (C-15), 26.6 (C-16), 16.2 (C-18), 15.9 (C-19), 23.1 (C-23), 125.8 (C-24), 131.0 (C-25), 25.8 (C-26), 17.9 (C-27), 28.0 (C-28), 16.5 (C-29), 17.3 (C-30), 105.0 (3-glc C-1′), 82.9 (C-2′), 77.2 (C-3′), 71.5 (C-4′), 78.0 (C-5′), 62.6 (C-6′), 105.6 (C-1″), 76.7 (C-2″), 78.8 (C-3″), 71.5 (C-4″), 78.0 (C-5″), 62.6 (C-6″), 97.9 (20-glc1 C-1′), 74.9 (C-2′), 78.6 (C-3′), 71.5 (C-4′), 76.7 (C-5′), 71.5 (C-6′), 105.0 (C-1″), 74.9 (C-2″), 78.0 (C-3″), 71.5 (C-4″), 78.0 (C-5″), 62.6 (C-6″).

Biological activity of ginsenosides

Initial screening for growth inhibition in vitro

Compounds **1**–**11** were tested for their in vitro anti-cancer activity using the MTT assay [43]. Four cell lines representing three types of human malignancies (breast, lung and prostate) were cultured with test compounds at concentrations in the range of 1–100 μM for 72 h, and cell viability was determined. The inhibitory effects of these compounds on cell growth are illustrated in Table 2. Of the 11 compounds, **1** (25-OH-PPD), **3** (PPD), and **5** (Rh_2) consistently showed substantial activity in all four cell lines. We subsequently evaluated the activity of these three compounds in comparison with compound **6** (Rg_3) and compound **2** (25-OH-PPT) in thirteen cell lines representing five types of human malignancies. Compound **2** and compound **6,** which is currently marketed as an anti-cancer agent in China [24], were used as controls. Although compound **2** has a structure similar to **1** and **3**, it showed minimal effects in most cells. In a dose-dependent manner, compounds **1** (25-OH-PPD), **3** (PPD), and **5** (Rh_2) inhibited the growth of all cell lines tested; IC_{50} values are listed in Table 3. For **1** (25(*S*)-OH-PPD), the IC_{50} values for most cell lines were in the range of 10–60 μM, demonstrating a 5–15-fold greater growth inhibition than Rg_3. The effects on growth by compounds **1**, **3** and **5** were similar, consistent with previous reports [30]. A representative comparison of growth inhibitory potential of the five compounds to lung cancer cells is shown in Fig. 2.

Induction of apoptosis in human cancer cells

In subsequent studies, we focused on lung cancer cell lines H838 and H358. As illustrated in Fig. 3, compounds **1** (25-OH-PPD), **3** (PPD), and **5** (Rh_2) induced apoptosis in a dose-dependent manner in both H838 (p53 wild-type) and H358 (p53 null) cell lines. At various concentrations, compound **1** consistently showed more potent effects relative to the other compounds. Compound **2** had minimal effects on apoptosis.

Table 2 Inhibition of growth of human cancer cells by compounds **1–11**

No.		MCF-7 Cells (CV%)			H838 Cells (CV%)			LNCaP Cells (CV%)			PC3 Cells (CV%)		
		1μM	10μM	100μM	1μM	10μM	100μM	1μM	10μM	100μM	1μM	10μM	100μM
1	25-OH-PPD												
2	25-OH-PPT												
3	PPD												
4	Daucosterol*												
5	Rh2												
6	Rg3												
7	Rg2												
8	Rg1												
9	Rd												
10	Re												
11	Rb1												

Cell viability (CV): inhibition <20%, in light gray; 20–90%, in dark gray; >90%, in black

*Highest concentration tested was 50 μM

Table 3 Growth inhibitory activity of five selected compounds (**1**, 25-OH-PPD; **2**, 25-OH-PPT; **3**, PPD; **5**, Rh_2 and **6**, Rg_3) in human cancer cells

Cancer type	Cell line	IC_{50} (μM)				
		25-OH-PPD	25-OH-PPT	PPD	Rh_2	Rg_3
Glioma	A172	49.4	>500	77.6	56.0	303.0
	T98G	27.5	125.9	72.8	71.8	397.0
Pancreatic	HPAC	22.5	>500	63.9	66.4	>500
	Panc-1	21.2	>500	30.2	41.3	180.3
Lung	A549	22.5	>500	27.2	33.9	369.1
	H1299	11.6	>500	20.3	20.4	357.2
	H358	22.9	>500	50.4	65.8	470.0
	H838	25.9	>500	77.4	64.4	293.0
Breast	MCF7	59.8	>500	68.4	41.5	361.2
	MDA-MB-468	68.7	>500	69.0	43.0	153.1
Prostate	LNCaP	35.7	>500	44.8	46.7	302.1
	PC3	59.8	>500	29.3	29.3	266.5

Inhibition of cell proliferation

In a dose-dependent manner, compounds **1**, **3**, **5**, and **6** inhibited cell proliferation (Fig. 4). The anti-proliferative effects were seen in both H838 (p53 wild type) and H358 (p53 null) cell lines. The effect of compound **2** on cell proliferation was minimal.

Cell cycle arrest in the G1 phase by compound **1**, *25(S)-OH-PPD*

In a dose-dependent manner, compound **1** (25-OH-PPD) induced cell cycle arrest in the G1 phase in both the H838 and H358 cell lines (Fig. 5). At various concentrations, compound **1** (with the highest

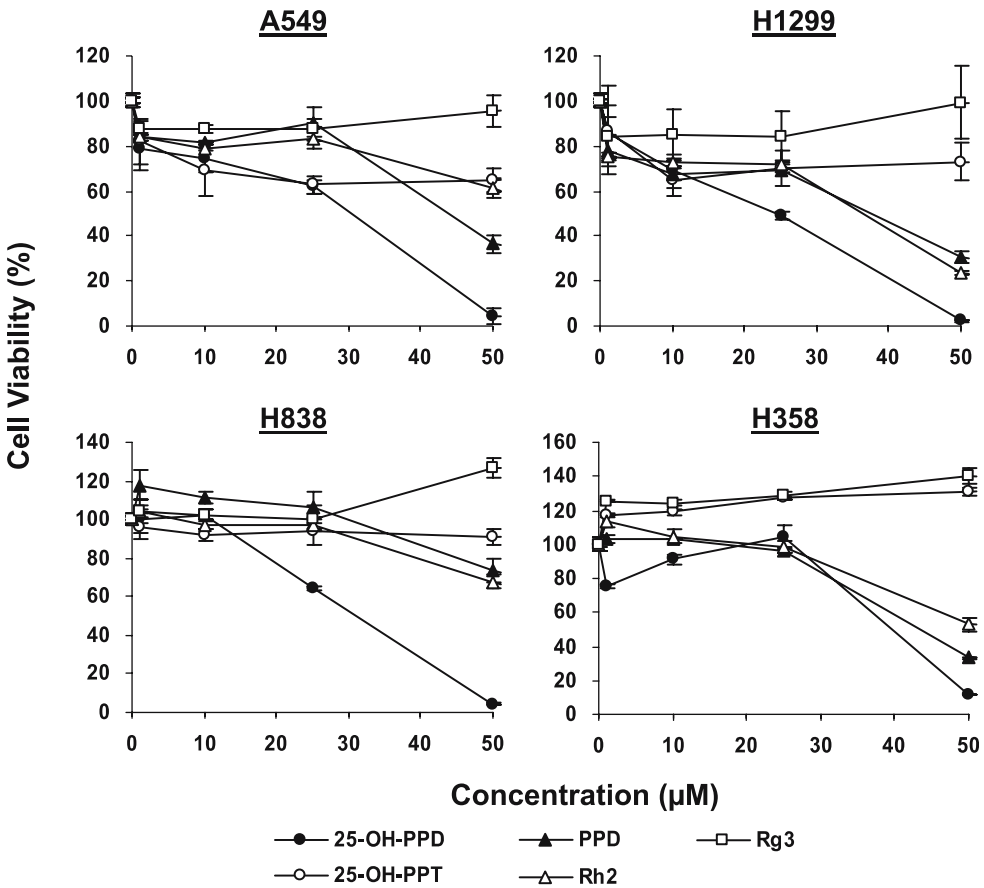

Fig. 2 Cytotoxicity of ginsenosides (**1**, 25-OH-PPD; **2**, 25-OH-PPT, **3**, PPD; **5**, Rh_2; and **6** Rg_3) to human lung cancer cells in culture. Percent viability is in comparison to untreated cells

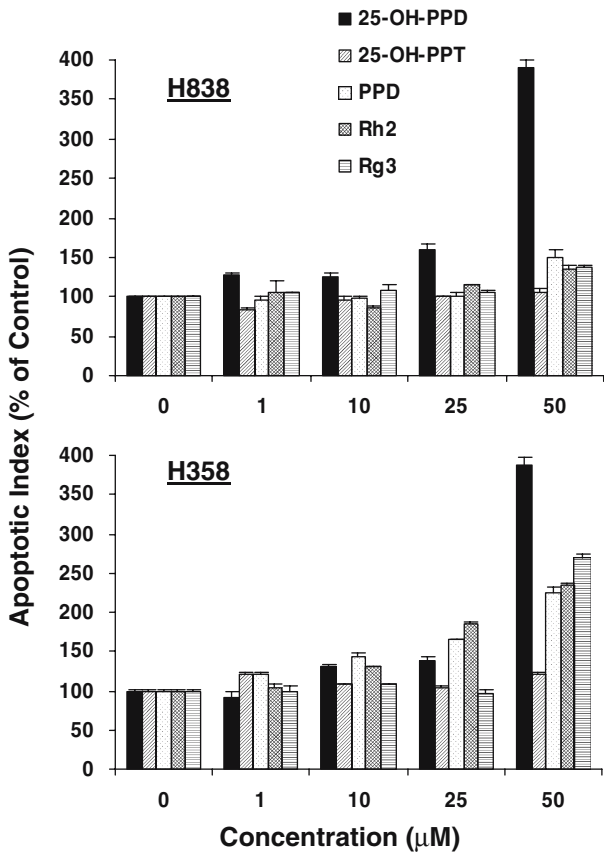

Fig. 3 Induction of apoptosis in lung cancer cells by ginsenosides (**1**, 25-OH-PPD; **2**, 25-OH-PPT; **3**, PPD; **5**, Rh_2 and **6**, Rg_3). The apoptotic index is in comparison to untreated cells

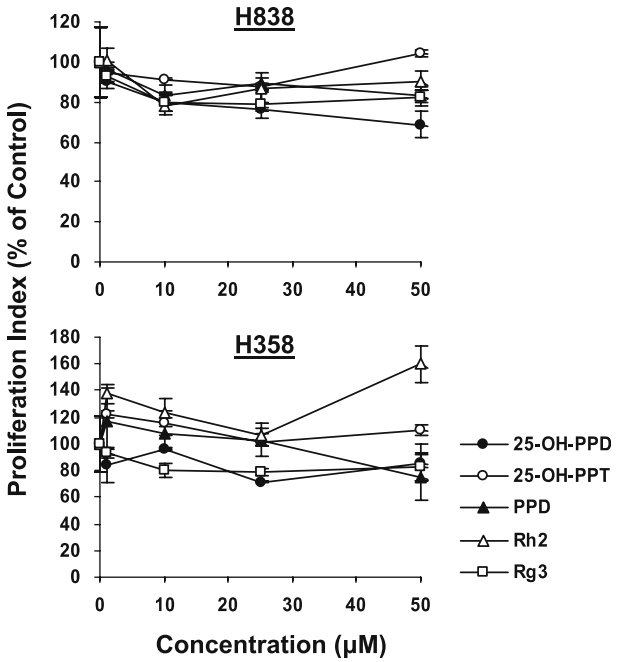

Fig. 4 Anti-proliferative effects of ginsenosides (**1**, 25-OH-PPD; **2**, 25-OH-PPT; **3**, PPD; **5**, Rh_2 and **6**, Rg_3) on human lung cancer cells in culture. The proliferative index is in comparison to untreated cells

concentration of 25 μM) consistently showed stronger effects in both cell lines, relative to the other compounds (with the highest concentration of 50 μM). Again, the effect of compound **2** was minimal.

Discussion

This is the first reported isolation of compounds **1**, **2**, **3**, **4**, **5**, **6** and **8** from the fruits of *P. ginseng*, indicating that the fruit of this plant may provide a novel source of these compounds. Numerous investigations have determined that the activities of ginsenosides are related to the types of aglycone and glycoside and the number of sugars linked to the core structure [40]. Previous studies of the structure–activity relationship of ginsenosides have shown that the activities of PPD compounds are greater than those of the PPT compounds, and that the aglycones are more effective than the glycosides. For example, ginsenosides Rh_1 (PPT type) and Rh_2 (PPD type), possessing sugar moieties at C-6 and C-3, respectively, have similar chemical structures, but their effects on B16 melanoma cells were remarkably different [26]. The activity of the various ginsenosides has been demonstrated to be in the order: monosaccharide glycoside > disaccharide glycoside > trisaccharide glycoside > tetrasaccharide glycoside, indicating that increasing the number of sugar moieties reduces the potency of the compound [8]. Further, both Rh_2 and Rh_1 (with a single sugar moiety) had anti-proliferative effects on human leukemia cells (THP-1), while Rg_3 (two sugar moieties) did not have a substantial anti-proliferative effect on the cells [30].

The present data further demonstrated this relationship. Compounds **1** (25-OH-PPD) and **3** (PPD) inhibited the growth of cancer cells, but a similar effect was not apparent for compound **6** (Rg_3) or for compounds **7**–**11**. Both compound **1** (25-OH-PPD) and compound **3** (PPD) increased apoptosis, but the effects of **5** (Rh_2) were less than those observed for **1** and **3**, showing that the presence of the sugar moiety attached to the Rh_2 structure reduces the ability of the ginsenoside to induce apoptosis. **1** also had stronger effect than **3** or **5** on cell growth inhibition, and its IC_{50} values (10–60 μM) were 5–15-fold lower than those for **6**, an agent already being marketed for cancer therapy [24]. Compounds **6**, **9** (Rd) and **11** (Rb_1) had little or no effect on cell growth and proliferation. These results indicate that specific differences in the ginsenoside chemical structure influence

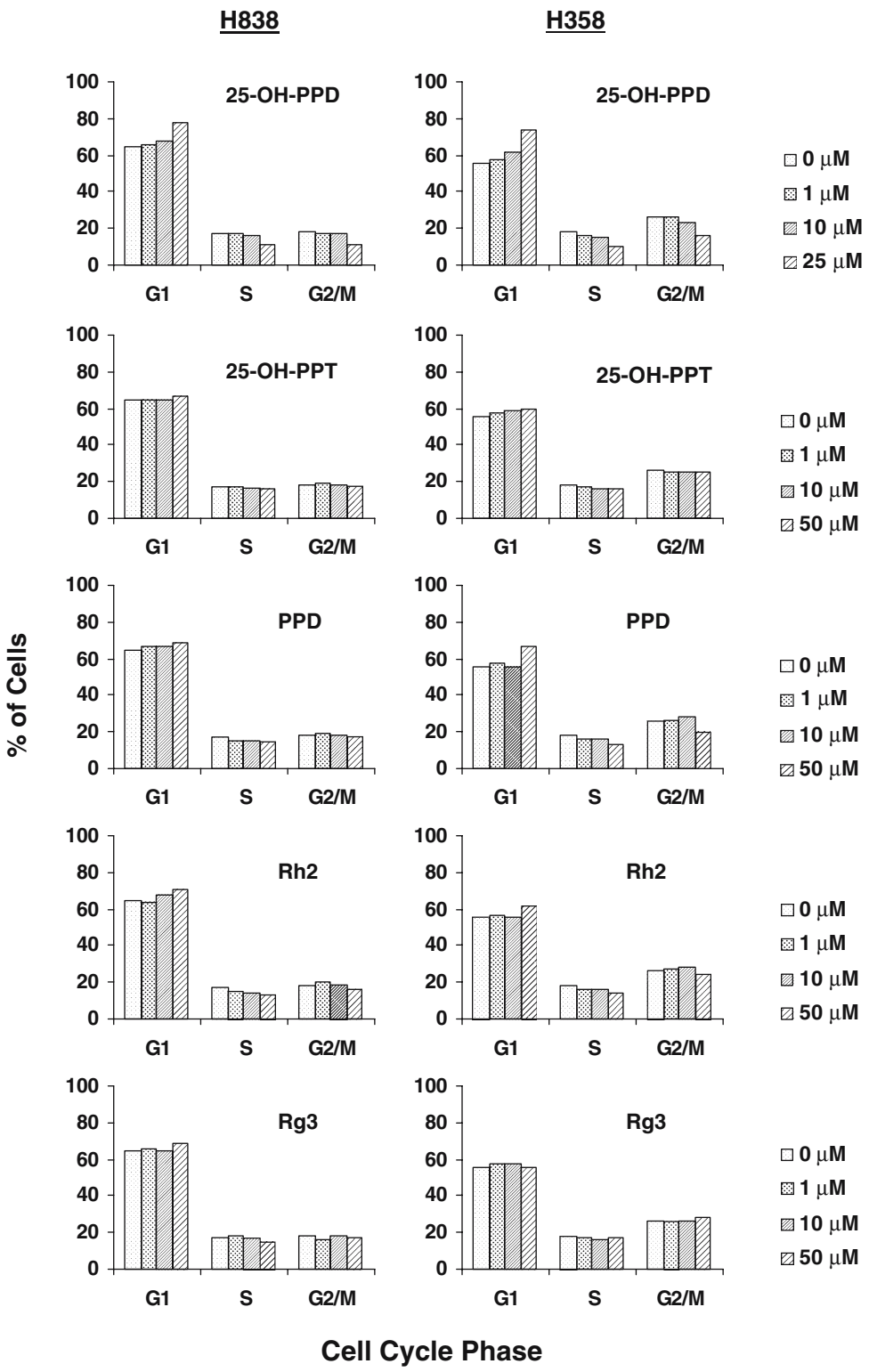

Fig. 5 Effect of ginsenosides on the cell cycle progression of lung cancer H838 and H358 cells in culture. Test compounds are **1**, 25-OH-PPD; **2**, 25-OH-PPT; **3**. PPD; **5**, Rh_2 and **6**, Rg_3

their cytotoxic properties. Although compound **1** was more effective than **3** or **5**, all three compounds (which are PPD-type saponins) were much more effective for inhibiting cancer cell growth and proliferation and increasing apoptosis than the PPT type saponins (compounds **2**, **7**, **8** and **10**). However, compound **1** was more effective for inducing apoptosis than the other compounds, suggesting that the different compounds may have different targets, resulting in different biological activities.

Thus our studies, and previous studies by other groups, of the SAR of the ginsenosides suggest that the structural type of dammarane saponin, the number of sugar moieties, and the substituent group(s) in the side chain of the aglycone affect their activity against cancer cells in culture. Our research results will be useful for evaluating the SAR of other ginsenosides and their aglycones, and possibly for developing novel agents that may be useful, especially as adjuvants, for the treatment of cancer.

In conclusion, we have isolated several ginsenosides from the fruits of *P. ginseng*, and have determined their structures on the basis of their physicochemical characteristics and NMR data. Several of the compounds have activity in a broad spectrum of human cancer cells. Although their mechanisms of action have yet to be elucidated, the notable activity of **1** (25-OH-PPD) may be associated with pathways involved in cell proliferation and cell cycle regulation, and more likely with apoptosis. With respect to the potency of these compounds, our results indicate that in vitro anticancer activities, such as the IC_{50} in cell cytotoxicity assays and the effective concentrations for inducing apoptosis, are similar to those observed with other natural products with demonstrated chemopreventive and chemotherapeutic activities, such as genistein [22]. Further molecular and pharmacological studies are underway in order to demonstrate the in vivo anti-tumor activity and elucidate the underlying mechanisms of action. The SAR results also will be helpful in developing synthetic ginsenoside derivatives or for using semi-synthetic approaches.

Acknowledgments We thank Dr. Haiyan Chen for excellent technical assistance, and Drs. Robert Diasio, Sam Lee, and Xianglin Shi for helpful discussion. Y. Zhao was supported by a Liaoning Modernization TCM grant (LN403004), People's Republic of China, and in part by LN Xinzhong Modern Medicine Co., Ltd. H. Wang was supported in part by the funds from the UAB Cancer Pharmacology Laboratory.

References

1. Akao T, Kanaoka M, Kobashi K (1998) Appearance of compound K, a major metabolite of ginsenoside Rb_1 by intestinal bacteria, in rat plasma after oral administration – measurement of compound K by enzyme immunoassay. Biol Pharm Bull 21:245–249
2. Attele AS, Wu JA, Yuan CS (1999) Ginseng pharmacology: multiple constituents and multiple actions. Biochem Pharmacol 58:1685–1693
3. Attele AS, Zhou YP, Xie JT, Wu JA, Zhang L, Dey L, Pugh W, Rue PA, Polonsky KS, Yuan CS (2002) Antidiabetic effects of Panax ginseng berry extract and the identification of an effective component. Diabetes 51:1851–1858
4. Bae EA, Han MJ, Kim EJ, Kim DH (2004) Transformation of ginseng saponins to ginsenoside Rh_2 by acids and human intestinal bacteria and biological activities of their transformants. Arch Pharmacal Res 27:61–67
5. Bae EA, Park SY, Kim DH (2000) Constitutive beta-glucosidases hydrolyzing ginsenoside Rb_1 and Rb_2 from human intestinal bacteria. Biol Pharm Bull 23:1481–1485
6. Bespalov VG, Alexandrov VA, Limarenko AY, Voytenkov BO, Okulov VB, Kabulov MK, Peresunko AP, Slepyan LI, Davydov VV (2001) Chemoprevention of mammary, cervix and nervous system carcinogenesis in animals using cultured Panax ginseng drugs and preliminary clinical trials in patients with precancerous lesions of the esophagus and endometrium. J Korean Med Sci 16:S42–S53
7. Chang YS, Seo EK, Gyllenhaal C, Block KI (2003) Panax ginseng: a role in cancer therapy? Integr Cancer Ther 2:13–33
8. Chen YJ, Wang HY, Xu SX et al (1995) Study on the chemical constituents of Panax ginseng and their structure–function relationship anti-arrythmia and anti-tumor. Science Foundation China 9:46–48
9. Cheng YJ, Su SX, Ma QF, Pei YP, Xie H, Yao XS (1987) Studies on new minor saponins isolated from leaves of Panax ginseng CA Meyer. Yao Xue Xue Bao 22:685–689
10. Dharmananda SI (2002) The nature of ginseng: traditional use, modern research and the question of dosage. Herbal Gram 54:343–351
11. Hasegawa H, Uchiyama M (1998) Antimetastatic efficacy of orally administered ginsenoside Rb_1 in dependence on intestinal bacterial hydrolyzing potential and significance of treatment with an active bacterial metabolite. Planta Med 64:696–700
12. Helms S (2004) Cancer prevention and therapeutics: Panax ginseng. Alternative Med Rev 9:259–274
13. Kennedy DO, Scholey AB (2003) Ginseng: potential for the enhancement of cognitive performance and mood. Pharmacol Biochem Behav 75:687–700
14. Keum YS, Han SS, Chun KS, Park KK, Park JH, Lee SK, Surh YJ (2003) Inhibitory effects of the ginsenoside Rg_3 on phorbol ester-induced cyclooxygenase-2 expression, NF-kappaB activation and tumor promotion. Mutat Res 523–524:75–85
15. Keum YS, Park KK, Lee JM, Chun KS, Park JH, Lee SK, Surh YJ (2000) Antioxidant and anti-tumor promoting activities of the methanol extract of heat-processed ginseng. Cancer Lett 150:41–48
16. Kim JY, Germolec DR, Luster MI (1990) Panax ginseng as a potential immunomodulator: studies in mice. Immonopharmacol Immunotoxicol 12:257–276
17. Kim TH, Lee YS, Cho CK, Park S, Choi SY, Yool SY (1996) Protective effect of ginseng on radiation-induced DNA double strand breaks and repair in murine lymphocytes. Cancer Biother Radiopharmaceut 11:267–272
18. Kitts DD, Hu C (2000) Efficacy and safety of ginseng. Pub Health Nut 4:473–485
19. Kitts DD, Wijewickreme AN, Hu C (2000) Antioxidant properties of North American ginseng extract. Mol Cell Biochem 203:1–10
20. Lee BH, Lee SJ, Hur JH, Lee S, Sung JH, Huh JD, Moon CK (1998) In vitro antigenotoxic activity of novel ginseng saponin metabolites formed by intestinal bacteria. Planta Med 64:500–503
21. Lee SJ, Ko WG, Kim JH, Sung JH, Moon CK, Lee BH (2000) Induction of apoptosis by a novel intestinal metabolite of ginseng saponin via cytochrome c-mediated activation of caspase-3 protease. Biochem Pharmacol 60:677–685

22. Li M, Zhang Z, Hill D, Chen X, Wang H, Zhang R (2005) Genistein, a dietary isoflavone, down-regulates the MDM2 oncogene at both transcriptional and posttranslational levels. Cancer Res 65:8200–8208
23. Li T S C (1995) Asian and American ginseng: a review. Hort Technology 5:27–34
24. Liu LW, Ye GC (2004) Clinical observation on inhibition of angiogenesis of thyroid cancer by Rg_3. Chin J Cancer Prev Treat 11:957–958
25. Nakata H, Kikuchi Y, Tode T, Hirata J, Kita T, Ishii K, Kudoh K, Nagata I, Shinomiya N (1998) Inhibitory effects of ginsenoside Rh_2 on tumor growth in nude mice bearing human ovarian cancer cells. Jap J Cancer Res 98:733–740
26. Odashima S, Ohta T, Kohno H, Matsuda T, Kitagawa I, Abe H, Arishi S (1985) Control of phenotypic expression of cultured B16 melaonma cells by plant glycosides. Cancer Res 45:2781–2784
27. Oh GS, Pae HO, Choi BM, Seo EA, Kim DH, Shin MK, Kim JD, Kim JB Chung HT (2004) 20(*S*)-Protopanaxatriol, one of ginsenoside metabolites, inhibits inducible nitric oxide synthase and cyclooxygenase-2 expressions through inactivation of nuclear factor-kappaB in RAW 264.7 macrophages stimulated with lipopolysaccharide. Cancer Lett 205:23–29
28. Ota T, Fujikawa-Yamamoto K, Zong ZP, Yamazaki M, Odashima S, Kitagawa I, Abe H, Arichi S (1987) Plant-glycoside modulation of cell surface related to control of differentiation in cultured B16 melanoma cells. Cancer Res 47:3863–3867
29. Park JA, Lee KY, Oh YJ, Kim KW, Lee SK (1997) Activation of caspase-3 protease via a Bcl-2-insensitive pathway during the process of ginsenoside Rh_2-induced apoptosis. Cancer Lett 121:73–81
30. Popovich DG, Kitts DD (2002) Structure–function relationship exists for ginsenosides in reducing cell proliferation and inducing apoptosis in the human leukemia (THP-1) cell line. Arch Biochem Biophys 406:1–8
31. Rhee YH, Ahn JH, Choe J, Kang KW, Joe C (1991) Inhibition of mutagenesis and transformation by root extracts of Panax ginseng in vitro. Planta Med 57:125–128
32. Sato K, Mochizuki M, Saiki I, Yoo YC, Samukawa K, Azuma I (1994) Inhibition of tumor angiogenesis and metastasis by a saponin of Panax ginseng, ginsenoside-Rb_2. Biol Pharmaceut Bull 17:635–639
33. Shibata S (2001) Chemistry and cancer preventing activities of ginseng saponins and some related triterpenoid compounds. J Korean Med Sci 16:S28–S37
34. Suh SO, Kroh M, Kim NR, Joh YG, Cho MY (2002) Effects of red ginseng upon postoperative immunity and survival in patients with state III gastric cancer. Am J Chinese Med 30:483–494
35. Wakabayashi C, Hasegawa H, Murata J, Saiki I (1997) In vivo antimetastatic action of ginseng protopanaxadiol saponins is based on their intestinal bacterial metabolites after oral administration. Oncol Res 9:411–417
36. Wang H, Cai Q, Zeng X, Yu D, Agrawal S, Zhang R (1999) Anti-tumor activity and pharmacokinetics of a mixed-backbone antisense oligonucleotide targeted to RIα subunit of protein kinase A after oral administration. Proc Natl Acad Sci USA 96:13989–13994
37. Wang H, Yu D, Agrawal S, Zhang R (2003) Experimental therapy of human prostate cancer by inhibiting MDM2 expression with novel mixed-backbone antisense oligonucleotides: In vitro and in vivo activities and mechanisms. Prostate 54:194–205
38. Wei TX, Chang LY, Wang JF, Edmund F, Morika J, Heinrich P, Chen WS, Eberhard B (1982) Zwei neue Dammarane-sapogenine aus den Blättern von Panax notoginseng. Plant Med 1982 45:167–171
39. Wu XG, Zhu DH, Li X (2001) Anticarcinogenic effect of red ginseng on the development of liver cancer induced by diethylnitrosamine in rats. J Korean Med Sci 16:S61–S65
40. Xie JT, Wang CZ, Wang AB, Wu J, Basila D, Yuan CS (2005) Antihyperglycemic effects of total ginsenosides from leaves and stem of Panax ginseng. Acta Pharmacol Sin 26:1104–1110
41. Yun TK, Choi SY (1995) Preventive effect of ginseng intake against various human cancers: a case-control study on 1987 pairs. Cancer Epidemiol Biomarkers Prev 4:401–408
42. Yun TK, Yun YS, Han IW (1983) Anticarcinogenic effect of long-term oral administration of red ginseng on newborn mice exposed to various chemical carcinogens. Cancer Detection Prev 6:515–525
43. Zhang Z, Li M, Wang H, Agrawal S, Zhang R (2003) Antisense therapy targeting MDM2 oncogene in prostate cancer: Effects on proliferation, apoptosis, multiple gene expression, and chemotherapy. Proc Natl Acad Sci USA 100:11636–11641
44. Zhao YQ, Yuan CL, Fu YQ, Wei XJ, Zhu HJ, Chen YJ, Wu LJ, Li X (1990) Chemical studies of minor triterpene compounds isolated from the stems and leaves of Panax ginseng CA Meyer. Yao Xue Xue Bao 25:297–301